

Competitive Binding Assay with an Umbelliferone-based Fluorescent Retinoid for Retinoid X Receptor Ligand Screening

Shoya Yamada, †, ‡, § Mayu Kawasaki, ¶ Michiko Fujihara, †, § Masaki Watanabe, † Yuta Takamura, † Maho Takioku, † Hiromi Nishioka, † Yasuo Takeuchi, † Makoto Makishima, || Tomoharu Motoyama, ¶ Sohei Ito, ¶ Hiroaki Tokiwa, #, Δ Shogo Nakano, ¶ and Hiroki Kakuta*, †*

†Division of Pharmaceutical Sciences, Okayama University Graduate School of Medicine, Dentistry and Pharmaceutical Sciences, 1-1-1, Tsushima-naka, Kita-ku Okayama 700-8530, Japan.

‡Research Fellowship Division, Japan Society for the Promotion of Science, Sumitomo-Ichibancho FS Bldg., 8 Ichibancho, Chiyoda-ku, Tokyo 102-8472, Japan.

§AIBIOS Co. Ltd. Tri-Seven Roppongi 8F 7-7-7 Roppongi, Minato-ku, Tokyo 106-0032 Japan.

||Division of Biochemistry, Department of Biomedical Sciences, Nihon University School of Medicine, 30-1 Oyaguchi-kamicho, Itabashi-ku, Tokyo 173-8610, Japan.

¶Graduate School of Integrated Pharmaceutical and Nutritional Sciences, University of Shizuoka, 52-1 Yada, Suruga-ku, Shizuoka 422-8526, Japan.

#Department of Chemistry, Rikkyo University, 3-34-1 Nishi-ikebukuro, Toshimaku, Tokyo 171-8501, Japan.

ΔResearch Center of Smart Molecules, Rikkyo University, 3-34-1 Nishi-ikebukuro, Toshima-ku, Tokyo 171-8501, Japan.

KEYWORDS. binding assay, fluorescence, retinoid X receptors, rexinoid, screening, umbelliferone

ABSTRACT. Ligands for retinoid X receptors (RXRs), “rexinoids”, are attracting interest as candidates for therapy of type 2 diabetes, Alzheimer’s and Parkinson’s diseases. However, current screening methods for rexinoids are slow and require special apparatus or facilities. Here, we created 7-hydroxy-2-oxo-6-(3,5,5,8,8-pentamethyl-5,6,7,8-tetrahydronaphthalen-2-yl)-2*H*-chromene-3-carboxylic acid (**10**, CU-6PMN) as a new fluorescent RXR agonist and developed a screening system of rexinoids using **10**. Compound **10** was designed based on the fact that umbelliferone emits strong fluorescence in a hydrophilic environment, but the fluorescence intensity decreases in hydrophobic environments such as the interior of proteins. The developed assay using **10** enabled screening of rexinoids to be performed easily within a few hours by monitoring changes of fluorescence intensity with widely available fluorescence microplate readers, without the need for processes such as filtration.

INTRODUCTION

There are 48 types of human nuclear receptors that regulate gene expression in response to binding of small-molecular ligands^{1,2}. Among them, retinoid X receptors (RXRs) often act as heterodimers with a variety of other receptors, and ligands targeting RXR (known as rexinoids³) can control the activities of these RXR heterodimers. Since RXRs are activated by low concentrations of 9-*cis* retinoic acid (**1**)⁴ (Figure 1), **1** had been considered as an endogenous ligand, though it has not been detected in blood⁵. More recently, 9-*cis*-13,14-dihydroretinoic acid (**2**) (Figure 1) has been suggested to be an endogenous ligand of RXR⁶. Many synthetic rexinoids have also been reported. Among them, bexarotene (**3**) (Figure 1) is an activator (agonist) of RXR and is used clinically to treat cutaneous T cell lymphoma (CTCL)⁷. It may also be effective against diabetes³, Alzheimer's disease^{8,9}, and Parkinson's disease^{10,11}. The basis of

these activities is thought to be activation of RXR heterodimers with nuclear receptors such as peroxisome proliferator-responsive receptors (PPARs), liver X receptor (LXR), and nuclear receptor related 1 protein (Nurr1), which are involved in the regulation of sugar and lipid metabolism, inflammation and other processes. The ability of RXR agonists to regulate these RXR heterodimers via their action on RXR alone is known as the permissive mechanism of activation¹². On the other hand, polyunsaturated fatty acids such as docosahexaenoic acid (DHA, **4**) (Figure 1) are natural rexinoids^{13,14}. They are reported to improve memory and metabolic syndrome¹⁵, and foods containing them are used as functional foods. Other compounds, including various environmental pollutants, can have adverse effects on nuclear receptors, for example serving as endocrine disruptors¹⁶. Therefore, there is a great demand for a simple, low-cost assay system that can identify compounds with RXR ligand activity, not only for drug discovery, but also for studies on functional foods and endocrine disruptors.

2) Time-resolved fluorescence resonance energy transfer (TR-FRET)¹⁷: This assay reveals recruitment of a co-activator peptide by test compounds within a short period. However, a special plate reader is required.

3) Binding assay using a radioisotope-labeled ligand¹⁸: This assay can assess the binding affinity of test compounds for RXR with high sensitivity, using a small amount of RXR peptide. However, this method requires a radioactive tracer (such as [³H]1), as well as bound/free (B/F) separation. The procedure is complicated and involves radioactivity-related safety issues.

4) Fluorescence quenching method (FQM)^{19,20}: This method is based on the quenching of autofluorescence derived from tryptophan in the ligand-binding site (LBD) of RXR. However, the autofluorescence of tryptophan is weak and the fluorescence wavelengths (Ex/Em 280/337 nm) are outside the range of usual plate readers.

Table 1. Existing Retinoid Search Technologies

	Measurement Principle	Advantages	Disadvantages
Reporter gene assay ⁴	Evaluation of transcriptional activation ability of test compounds using overexpressing RXRs	Transcription activation by test compounds can be measured.	A long time is required (3–4 days).
Time-resolved fluorescence resonance energy transfer (TR-FRET) ¹⁷	FRET phenomenon between a terbium-labeled RXR and a coactivator labeled with fluorescein	Activation of RXR by test compounds can be measured in a short period.	A special plate reader is required for TR-FRET.
Binding assay using radiolabelled compound (ex. [³ H]1) ¹⁸	Based on competition of test compounds and radio-labeled compound for binding to RXRs	Highly sensitive. Small amount of receptor protein is sufficient.	Bound/free (B/F) separation is necessary, the procedure is complicated, & safety issues.
Fluorescence quenching	Binding of test compound quenches the autofluorescence of	Measurement can be done just by	Usual plate readers are not

method (FQM) ^{19,20}	tryptophan in RXRs.	mixing RXR-LBD and test compound.	suitable (Ex/Em 280/337 nm are outside usual range & auto fluorescence is weak).
----------------------------------	---------------------	--------------------------------------	---

Other reported RXR ligand screening methods include cell-based RXR assays such as a yeast reporter assay²¹; magnetic microbead affinity selection screening (MagMASS) to find RXR ligands in complex mixtures^{22,23} and virtual screening approaches for RXR ligands²⁴. However, cell-based RXR assays require a long time (3–4 days). MagMASS requires HPLC-MS apparatus. As for virtual screening, it is always necessary to experimentally confirm the binding affinity of candidate RXR ligands.

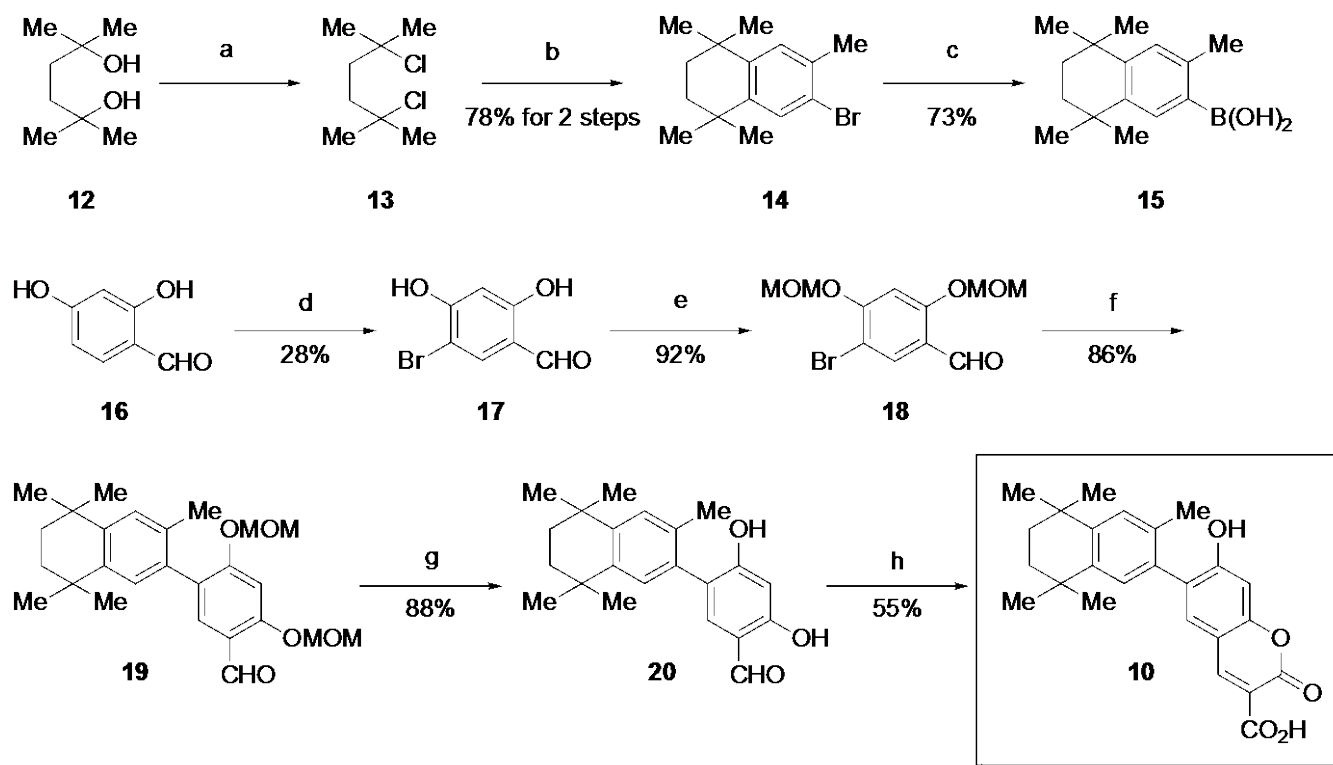
Thus, to overcome the disadvantages of existing methods, we set out to design a fluorescent rexinoid that would be suitable for use in a simple, highly sensitive RXR binding assay. We previously reported the fluorescent RXR agonist **5** (Figure 1), which has a fluorescent carbostyryl structure **6** in place of the 1,1,4,4-tetramethyltetralin structure of **3**. Compound **5** has been used in a fluorescence polarization-based assay targeting RXRs.²⁵ However, the RXR agonist activity of **5** was much weaker than that of **3** (the EC₅₀ values were 1 μ M and 20 nM, respectively), and its relatively poor binding ability to RXRs was a significant drawback. Therefore, in this study, we aimed to create a new fluorescent RXR agonist that would be suitable for highly sensitive RXR ligand screening using a standard fluorescence plate reader.

RESULTS AND DISCUSSION

Pohl et al. reported fluorescent retinoids targeting cellular retinoid binding protein II (CRABP II)^{26,27}. Compared to CRABP II, less space is available in the ligand-binding site of RXR²⁵, and therefore we considered that the acidic domain of RXR agonists would have to be converted to a fluorophore.

Umbelliferone (**7**) is a fluorophore that can be detected with a widely available fluorescent filter set (Ex 360 nm/ Em 465 nm)²⁸. Its derivative **8** with a carboxy group at the 3-position has a 7-hydroxyl group, which exists in OH form in a hydrophobic environment, but as the anion (O⁻) in an aqueous environment, resulting in an increase of fluorescence intensity²⁹. Thus, if the receptor-bound compound is displaced by a competitively binding RXR ligand, an increase of the fluorescence intensity will be observed. With this in mind, we designed and synthesized **10** (Design 1), which has an umbelliferone skeleton, and its regioisomer **11** (Design 2) based on the chemical structure of the RXR agonist CD3254 (**9**).³⁰ Since **9** has a cinnamic acid structure, we anticipated that this structure could be developed towards an umbelliferone structure. Compounds **10** and **11** were synthesized according to Schemes 1 and 2.

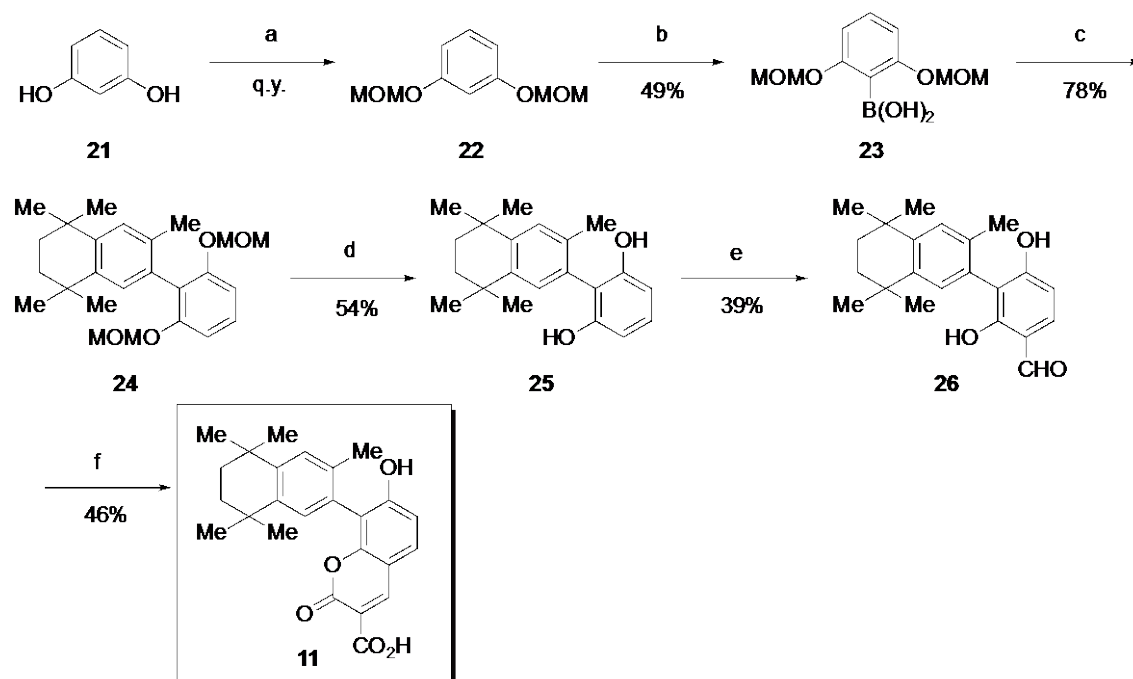
Scheme 1.^a



Reagents and conditions: a) conc. HCl, b) 2-bromotoluene, AlCl₃, DCM, 78% for 2 steps. c) 1) *n*-BuLi, B(O*i*-Pr)₃, THF. 2) 2 M HCl, 73%. d) Br₂, AcOH, 28%. e) MOMCl, DIPEA, DMF, 92%. f) 4,

Pd(PPh₃)₄, 2 M Na₂CO₃, EtOH, toluene, 86%. g) 4 M HCl/EtOAc, 88%. h) Meldrum's acid, piperidine, EtOH, 55%.

Scheme 2.^a



Reagents and conditions: a) MOMCl, NaH, DMF, q.y. b) 1) *n*-BuLi, Et₂O, 2) B(OMe)₃, 49%. c) **14**, Pd(PPh₃)₄, K₃PO₄, DME, H₂O, 78%. d) 4 M HCl/EtOAc, 54%. e) POCl₃, DMF, 39%. f) Meldrum's acid, piperidine, EtOH, 46%.

In reporter assay, **10** showed potent RXR activation ($EC_{50} = 22$ nM toward human RXR α), like **3** (Figure 2A). In binding assay using human RXR α ligand-binding domain (hRXR α -LBD), both compounds showed concentration-dependent competition with [³H]**1** (Figure 2B). The IC₅₀ values were calculated from the binding data, and the inhibition constant (K_i) of each compound was determined using the Cheng-Prusoff equation.³¹ The K_i values for **3** and **10** were 150 nM and 230 nM, respectively. However, the behavior of **10** was different from that of **3**, in that [³H]**1** was not completely displaced

from the receptor by **10**. In addition, at the lower concentration of **10**, the % of bound [^3H]**1** was increased compared to that in the absence of **10** as a competitor.

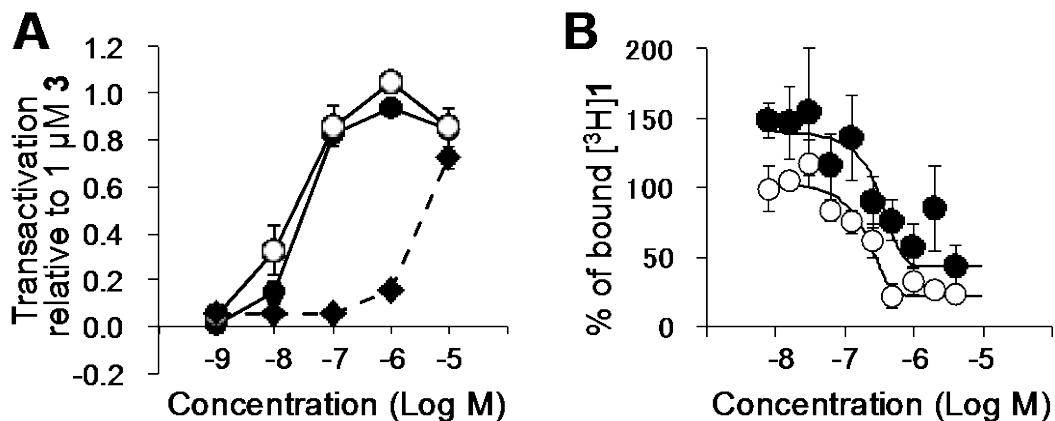


Figure 2. Transactivation of human RXR α (hRXR α) by **3**, **10** and **11** and binding to human RXR α ligand-binding domain (hRXR α -LBD) of **3** and **10** in the presence of [^3H]**1**. (A) Dose-dependent agonistic activity curves of **3** (open circles), **10** (closed circles) and **11** (closed diamonds) toward hRXR α in COS-1 cells. The data are shown as relative transactivation activity with respect to 1 μM **3**, taken as 1. Data are mean \pm SD ($n = 3$). (B) Dose-dependent binding of [^3H]**1** with hRXR α -LBD in the presence of **3** (open circles) or **10** (closed circles). The data are shown as % of the value of [^3H]**1** in the absence of any competitive sample. [^3H]**1** and hRXR α -LBD were used at concentrations of 10 nM and 50 nM, respectively. Data are mean \pm SD ($n = 3$).

To reveal the reason for these incongruities, we conducted X-ray structure analysis. The crystal structure of the hRXR α -LBD/**10** (green) complex was determined at 2.65 \AA resolution (Figure 3, Table S1) (PDB code 6JNO). The structure turned out to be tetrameric and the coupling ratio of **10** to RXR α -LBD was predicted as 4 to 2 based on the electron density map of hRXR α -LBD/**10** complex. In addition, this confirmed that **10** binds at the dimer-dimer interface, in contrast to **1** (PDB ID: 3OAP),³² and this

may be the reason why [³H]**1** was not completely displaced from the receptor by **10**. Though ligand-binding at the dimer-dimer interface has already been reported for RXR antagonists rhenin (PDB ID: 3R2A),³³ K8003 (PDB ID: 5TBP),³⁴ and K8008 (PDB ID: 4N8R)³⁵ (Figure S1), this is the first example of an RXR agonist binding at this location. Since **10** has RXR agonist activity and showed concentration-dependent competition with [³H]**1**, it seems likely that **10** also binds to the ligand-binding pocket (LBP) of the hRXR α -LBD, like **3**, as well as to the dimer-dimer interface. However, it is still not clear why a low concentration of **10** promoted the binding of [³H]**1**. One possibility might be that binding of **10** to the interface induces some structural change at the LBP.

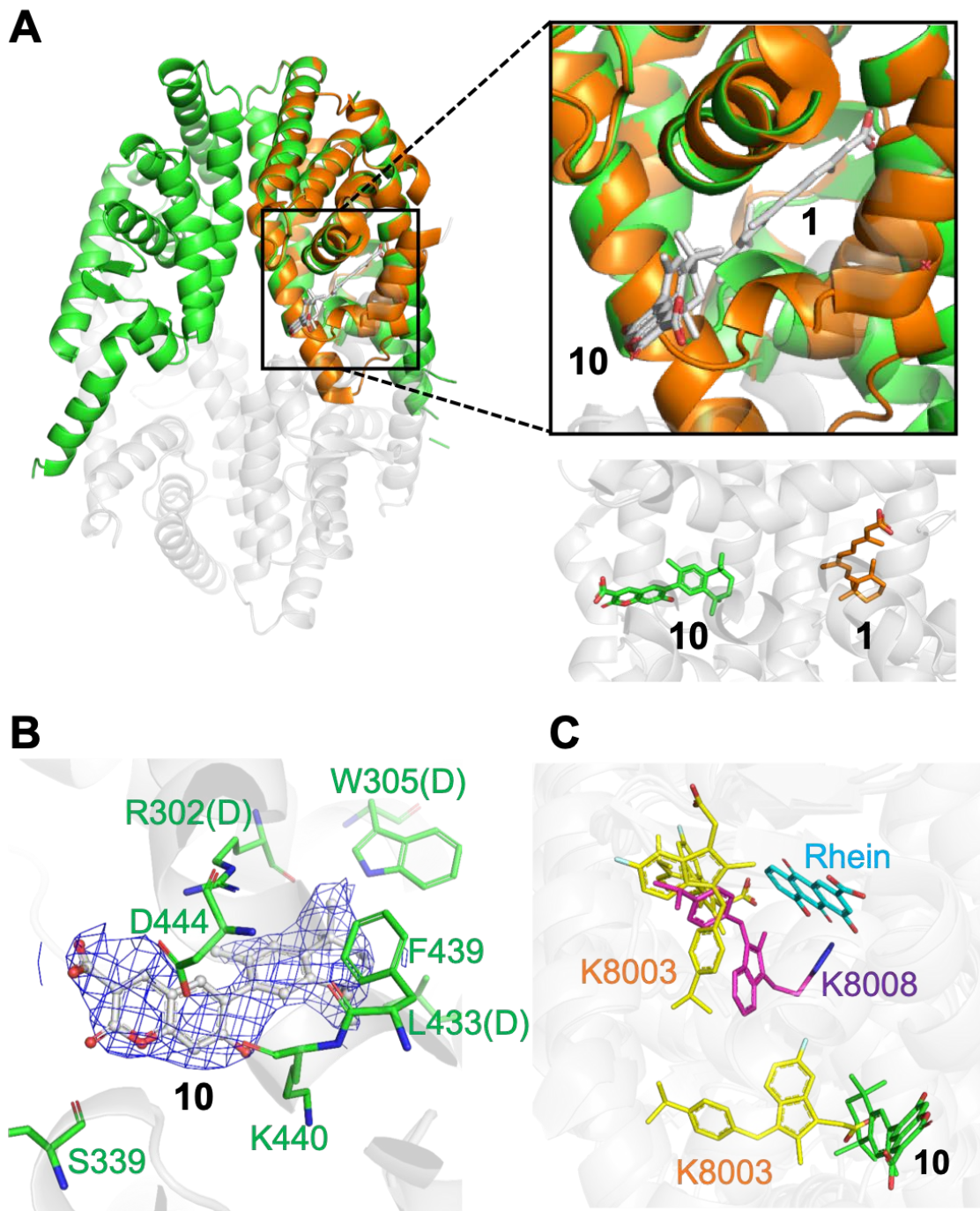


Figure 3. Structure of the complex of **10** with the hRXR α -LBD. (A) Comparison of ligand-binding modes in hRXR α -LBD. The hRXR α -LBD in the complexes with **10** (PDB ID: 6JNO) and **1** (PDB ID: 3OAP)³² is shown in green and orange, respectively. The binding site of **10** to the hRXR α -LBD is located at the interface between the two domains of the hRXR α -LBD. (B) The 2Fo-Fc electron density map (blue color) was contoured at 0.50 σ . (C) Comparison of ligand-binding modes in hRXR α -LBD.

The binding modes of rhein (PDB ID: 3R2A),³³ K8003 (PDB ID: 5TBP),³⁴ K8008 (PDB ID: 4N8R),³⁵ and **10** are shown in cyan, magenta, yellow and green, respectively.

The fluorescence properties of **10** were examined. The maximum absorbance of **10** in 0.1 N aqueous solution of sodium hydroxide was 396 nm, the maximum fluorescence wavelength was 453 nm, and the fluorescence quantum yield was 0.47 (Table 2, Figure S2). In addition, when the fluorescence intensity was measured with fixed excitation and fluorescence wavelengths (Ex 360 nm/ Em 465 nm) in several solvents with different polarity, the fluorescence intensity of **10** decreased significantly as the solvent polarity decreased (Figure 4B). This suggests that a decrease in the fluorescence intensity of **10** can be expected upon binding to RXR, due to the more hydrophobic environment, as anticipated. Thus, the binding ability of **10** to RXR was determined based on the change in the fluorescence intensity of **10** upon binding to the hRXR α -LBD (Figure 4C). The experimental protocol is described in the supporting information. After sample mixing at room temperature, the measured intensity became stable at 2 hours, so all fluorescent measurements were made under these conditions. The fluorescence intensity of **10** decreased in a sigmoid manner depending on the concentration of hRXR α -LBD (Figure 4C), and a Hill coefficient (*n*) of 1.9 and dissociation constant (*K_d*) of 233 nM were obtained (Figure 4D). A Hill coefficient of >1 indicates positive cooperativity, i.e., binding of the first ligand facilitates binding of a second ligand at another site on the dimeric receptor complex. Imai et al. reported similar results for a fluorescent ligand targeting the homodimeric estrogen receptor.³⁶ The fact that the Hill coefficient is greater than 1 implies that binding of **10** to RXRs induces positive cooperativity, i.e., binding of **10** to RXRs induces further binding of **10**.

Table 2. Absorption and Fluorescence Data of 10 in 0.1 N NaOH and MeOH, respectively

Solvent	ϵ	λ_{Abs}	λ_{Em}	Φ
	[L/(mol·cm)]	[nm]		
0.1 N NaOH	1.78×10^4	396	453	0.468 ± 0.003
MeOH	6.71×10^3	352	453	0.095 ± 0.02

n = 3, mean \pm SD

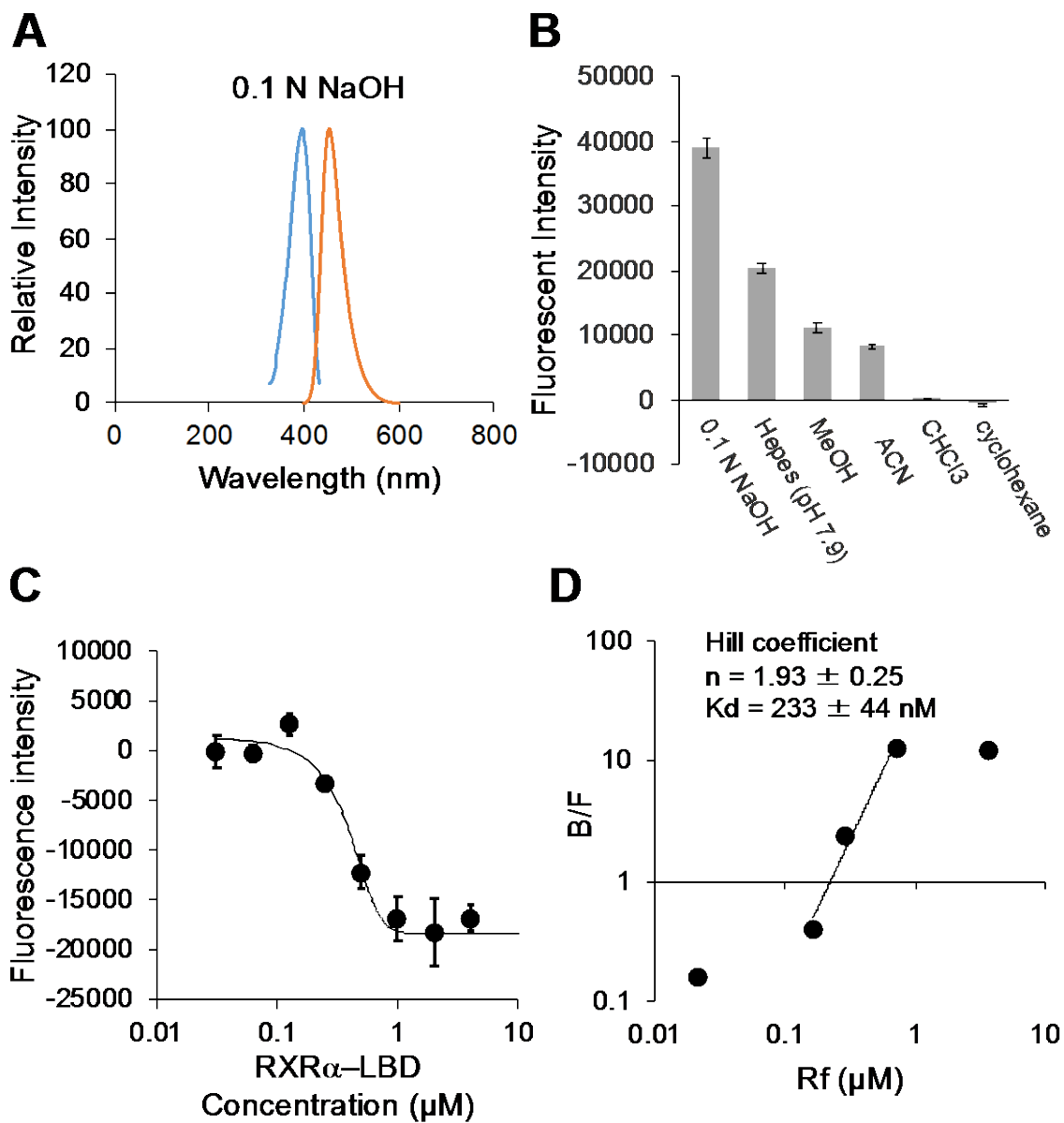


Figure 4. Characterization of **10**. Relative absorbance and fluorescence spectra of **10** in 0.1 N NaOH.

(A) Fluorescence spectra were obtained at Ex/Em = 396 nm/453 nm. (B) Relative fluorescent intensity

data of 100 nM **10** in various solvents containing 1% DMSO (Ex/Em = 360 nm/465 nm). (C and D) Specific binding curve (C) and Hill plot (D) of **10** with hRXR α -LBD. “Rf” is the concentration of free receptor. Final concentration of **10** was 300 nM in assay buffer containing 10 mM Hepes, 150 mM NaCl, 2 mM MgCl₂, 5 mM DTT (pH7.9). DMSO final concentration was 1%. Ex/Em=360 nm/465 nm. Data are mean \pm SD (n = 4).

Next, the affinity of test compounds for RXR was determined using **10** and hRXR α -LBD in a 384-well plate. To each well (4 wells per sample), 10 μ L of hRXR α -LBD at 1 μ M (final concentration 0.5 μ M), 5 μ L of the sample at 4 times higher concentration than the final concentration, and 5 μ L of 400 nM **10** (final concentration 100 nM) were added. The mixture was incubated for 2 hours at room temperature and the fluorescence intensity was measured. This incubation time was chosen based on evaluation of the Z'-factor at incubation times of 0.5, 1, 2, 3 hours for **10** and hRXR α -LBD (Figure S3). The IC₅₀ was calculated from the fluorescence intensity data, and the K_i of each compound was determined using the Cheng-Prusoff equation.³¹ The experimental protocols and data analysis methods are described in the supporting information. The K_i values are shown in Table S2. Figure 5A compares the results of radioisotope (RI) experiments using [³H]**1** and the assay using **10** to measure the binding ability of known rexinoids to hRXR α -LBD (Figures S4 and S5). Because of limited availability, we used commercially available hRXR α -LBD for the RI experiment, and our prepared protein for the binding assay using compound **10**. The correlation coefficient between K_i values determined by the two methods was about 0.7, despite the difference in hRXR α -LBD preparation used. However, rexinoids that gave small K_i values in RI, such as NEt-3IB (Figure S4), gave K_i values one order of magnitude higher as determined in the assay using **10**. The reason for this is not clear, but might be related to failure of **10** to completely displace [³H]**1**, observed in the RI experiments. Because polyunsaturated fatty acids are known to function as rexinoids^{13,14}, their binding ability to RXR was also examined using the developed method (Figure 5B and Table S3). A higher concentration of DHA (**4**) was required for

binding to RXR, compared to bexarotene (**3**), while no binding of palmitic acid was observed, in accordance with previous reports.³⁷ Interestingly, our system revealed the binding affinity of eicosapentaenoic acid (EPA), which has not reported before. We also evaluated some readily available RXR antagonists using this method and confirmed the order of binding affinity (Figures S6 and S7, and Table S3). Thus, our system provides simple and sensitive methodology with readily available equipment for the initial screening of RXR ligands, though the agonistic or antagonistic activity of hits would need to be separately examined.

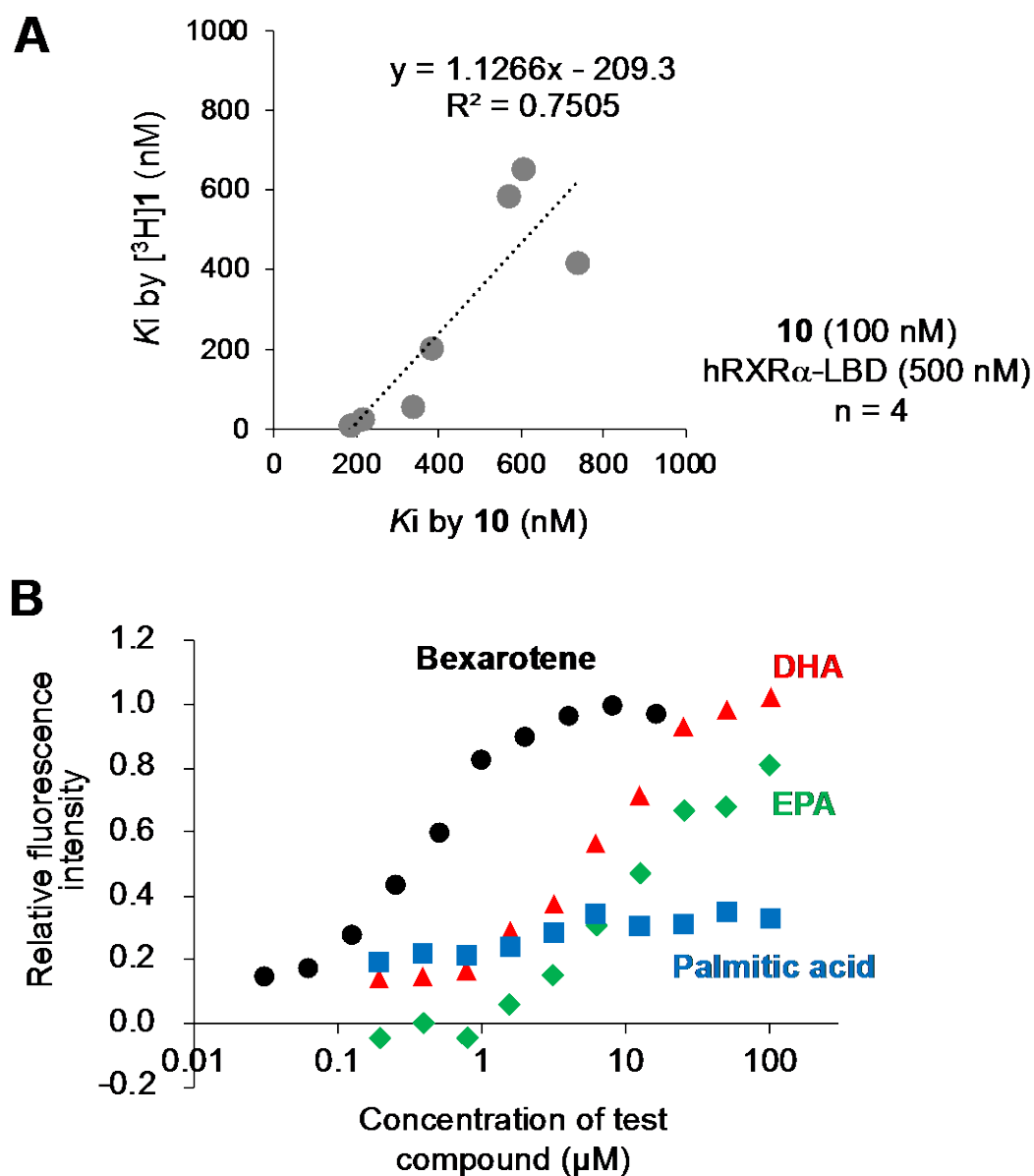


Figure 5. Competitive binding assay using **10**. (A) Correlation of hRXR-LBD binding affinity values obtained with **10** and [³H]**1**. The K_i values obtained with **10** and those obtained with [³H]**1** are plotted on the X and Y axes, respectively. (B) Relative fluorescence intensity curves of test compounds in the assay using **10**. These data were calculated by subtraction of the fluorescence values for the hRXR α -LBD with the test compound in the absence of **10** from those in the presence of **10**. The y-axis is shown as the relative value to 10 μ M **3**, taken as 1 (positive control). This assay was performed in a 384-well plate (4 wells/sample). Final concentrations of **10** and hRXR α -LBD were 100 nM and 500 nM, respectively. Each compound except for **3** was added at 0.20, 0.39, 0.78, 1.56, 3.13, 6.25, 12.5, 25, 50 and 100 μ M (final concentration). Assay buffer contained 10 mM Hepes, 150 mM NaCl, 2 mM MgCl₂, 5 mM DTT (pH 7.9). DMSO final concentration was 1%. Ex 360 nm/Em 465 nm. Data are mean \pm SD (n = 4).

CONCLUSIONS

In this study, we designed and synthesized an umbelliferone derivative **10** as a new fluorescent rexinoid, and applied it to develop a fluorescence-based RXR-binding assay system for screening rexinoids. This assay system is simple, sensitive, and can be performed in a few hours with widely available fluorescence microplate readers, without the need for processes such as filtration. Though there remains an issue concerning the correlation of this assay system with RI experiments, this assay is expected to be useful for simple, rapid, low-cost screening studies. Hit compounds can then be followed up by assessing transcriptional activity by means of reporter gene assay. We believe it will be useful not only for identifying RXR binders in drug discovery studies, but also for studies of functional foods and endocrine disruptors, though it should be noted that fluorescence-based assays often suffer from interference when used to screen natural products. A similar strategy may also be applicable to other receptors.

EXPERIMENTAL SECTION

Chemistry.

General. All solvents and chemicals were used as purchased without further purification. The progress of all reactions was monitored by thin layer chromatography (TLC) on 0.2 mm thick TLC plates (Merck, glass-backed, silica gel 60 F245), and spots were detected under UV light. Silica gel 60 (Kanto Chemical, particle size 0.04–0.05 mm) was used for purification by flash column chromatography. ^1H NMR and ^{13}C NMR spectra were measured on a Varian Mercury-300 (^1H 300 MHz, ^{13}C 75 MHz) spectrometer or a Varian VXR-400 (^1H 400 MHz) spectrometer at room temperature. Deuterated chloroform and dimethyl sulfoxide (CDCl_3 and $\text{DMSO-}d_6$) were used as solvents in all routine NMR measurements. Chemical shifts are reported in ppm relative to the respective deuterated solvent peak, CHCl_3 (δ 7.26 ppm), $\text{DMSO-}d_6$ (δ 2.50 ppm) for ^1H NMR and CDCl_3 (δ 77 ppm) for ^{13}C NMR, and coupling constants are given in Hz. FAB-MS spectra were measured on a JEOL JMS-700 mass spectrometer. Electrospray ionization (ESI) mass spectra were measured on a Bruker MicrOTOF. Melting points were determined with a J-Science RFS-10 hot stage microscope. Elemental analysis was carried out with a Perkin Elmer 2400 Series II CHNS/O Elemental Analyzer and results were within \pm 0.4% of the theoretical values. The purity of all tested compounds was $>95\%$, as confirmed by HPLC.

Preparative HPLC. Preparative HPLC was performed using a Shimadzu liquid chromatographic system (Kyoto, Japan) consisting of an LC-10AS pump, SPD-10AV UV–vis spectrophotometric detector, CTO-10AS column oven and C-R5A Chromatopac. The samples (2 mL) were injected and the chromatographic analyses were carried out on an YMC Pack ODS-AM (10 mm i.d. \times 250 mm, 5 μm , YMC Co., Ltd.) at 40 $^\circ\text{C}$, using $\text{MeOH}:\text{H}_2\text{O}$ (85/15 + 0.1% formic acid, v/v) as the mobile phase. The flow rate was 0.7 mL/min and the absorbance at 260 nm was monitored. All the solvents were of analytical grade and were used directly without purification.

Analytical HPLC. Analytical HPLC was performed using a Shimadzu liquid chromatographic system (Kyoto, Japan) consisting of an LC-10AD pump, SPD-10AV UV–vis spectrophotometric detector, CTO-10AS column oven and C-R5A Chromatopac. The samples (each 20 μ L) were injected onto an Inertsil ODS-3 (4.6 i.d. \times 100 mm, 3 μ m, GL Sciences, Tokyo, Japan) fitted with a guard column of Inertsil ODS-3 (4.0 mm i.d. \times 10 mm, 3 μ m, GL Sciences) at 40 $^{\circ}$ C, using MeOH:H₂O (85/15 + 0.1% formic acid, v/v) as the mobile phase. The flow rate was 0.7 mL/min and the absorbance at 260 nm was monitored.

7-Hydroxy-2-oxo-6-(3,5,5,8,8-pentamethyl-5,6,7,8-tetrahydronaphthalen-2-yl)-2H-chromene-3-carboxylic acid (10, CU-6PMN). To a solution of **20** (41 mg, 0.12 mmol) and Meldrum's acid (17 mg, 0.12 mmol) in ethanol (1 mL) was added piperidine (50 μ L). The reaction mixture was refluxed for 2 h, then poured into water (30 mL), acidified with sat. NH₄Cl aq and extracted with EtOAc (2 \times 100 mL). The organic layer was washed with water (2 \times 50 mL) and brine (50 mL), dried over Na₂SO₄, and filtered. The filtrate was evaporated in a rotary evaporator. The residue was recrystallized from CH₂Cl₂/MeOH to yield 27 mg of **10** as a yellow particulate solid (55%). Mp: 229.6–230.1 $^{\circ}$ C ¹H-NMR (300 MHz, DMSO-d₆) δ : 8.70 (s, 1H), 7.63 (s, 1H), 7.18 (s, 1H), 7.03 (s, 1H), 6.85 (s, 1H), 2.05 (s, 3H), 1.65 (s, 4H), 1.27 (s, 6H), 1.22 (s, 6H). ¹³C-NMR (75 MHz, CDCl₃) δ : 165.07, 163.81, 161.22, 156.61, 151.86, 147.10, 144.34, 134.33, 132.46, 130.14, 129.57, 129.03, 128.88, 112.70, 111.17, 103.66, 51.30, 45.42, 35.29, 35.26, 34.62, 34.46, 32.30, 32.17, 19.78. FAB-MS m/z: 407 [M + H]⁺. HRMS (ESI⁻) m/z: [M – H]⁻ Calcd for C₂₅H₂₅O₅ 405.1707; Found 405.1704. Anal. Calcd for C₂₅H₂₆O₅·1/4H₂O: C, 73.06; H, 6.50. Found: C, 72.69; H, 6.13. Analytical HPLC: 9.8 min; >95% purity.

7-Hydroxy-2-oxo-8-(3,5,5,8,8-pentamethyl-5,6,7,8-tetrahydronaphthalen-2-yl)-2H-chromene-3-carboxylic acid (11). To a solution of **26** (18 mg, 0.053 mmol) and Meldrum's acid (8.0 mg, 0.053 mmol) in ethanol (1 mL) was added piperidine (50 μ L). The reaction mixture was refluxed for 2 h, then poured into water (30 mL). The mixture was acidified with 2 M HCl aq and extracted with EtOAc (2 \times 50 mL). The organic layer was washed with water (2 \times 50 mL) and brine (50 mL), dried over Na₂SO₄,

and filtered. The filtrate was evaporated in a rotary evaporator. The residue was chromatographed (SiO₂, EtOAc/*n*-hexane = 1/3, v/v) to yield 20 mg of a yellow solid, which was further purified by preparative HPLC (MeOH/H₂O = 85/15 + 0.1% formic acid, v/v). The eluate was evaporated under reduced pressure to afford 10 mg of **11** as a pale-yellow solid (46%). Mp: 221.7–223.0 °C ¹H-NMR (300 MHz, CDCl₃) δ: 8.92 (s, 1H), 7.68 (d, 1H, *J* = 8.8 Hz), 7.32 (s, 1H), 7.16 (d, 1H, *J* = 8.8 Hz), 7.10 (s, 1H), 2.06 (s, 3H), 1.72 (s, 4H), 1.37 (s, 3H), 1.33 (s, 3H), 1.26 (s, 6H). ¹³C-NMR (75 MHz, CDCl₃) δ: 164.67, 163.34, 160.63, 155.83, 151.80, 146.97, 144.00, 134.72, 131.23, 129.55, 128.54, 124.10, 116.64, 114.99, 112.47, 110.44, 34.92, 34.83, 34.23, 34.05, 32.02, 31.81, 31.76, 31.70, 19.31. FAB-MS *m/z*: 407 [M + H]⁺. HRMS (ESI⁻) *m/z*: [M – H]⁻ Calcd for C₂₅H₂₅O₅ 405.1707; Found 405.1704. Anal. Calcd for C₂₅H₂₆O₅·3/2H₂O: C, 69.26; H, 6.76. Found: C, 69.65; H, 6.79. Analytical HPLC: 8.8 min; >97% purity.

6-Bromo-1,1,4,4,7-pentamethyl-1,2,3,4-tetrahydronaphthalene (14). This compound was prepared according to references 38 and 39. 2,5-Dimethyl-2,5-hexanediol (**12**, 2.0 g, 13.6 mmol) was dissolved in conc. HCl (20 mL) and the solution was stirred at room temperature for 4 h. The mixture was filtered. The filtrate was washed with water and dissolved in CH₂Cl₂ (150 mL) and the organic solution was washed with water (50 mL). The resulting solution was dried over MgSO₄, filtered, and evaporated using a rotary evaporator to afford **13**. Then **13** was dissolved in CH₂Cl₂ again, and 2-bromotoluene (3.3 mL, 27 mmol) was added to the solution. Next, AlCl₃ (170 mg) was slowly added at 0 °C under Ar. The reaction mixture was stirred at room temperature for 20 h, and then diluted with *n*-hexane (150 mL). The organic layer was collected, washed with water (2 × 50 mL) and brine (50 mL), dried over MgSO₄, and filtered. The filtrate was evaporated in a rotary evaporator, and the residue was recrystallized from methanol to yield 3.0 g of **14** as yellow needles (78%). ¹H-NMR (300 MHz, CDCl₃) δ: 7.42 (s, 1H), 7.14 (s, 1H), 2.34 (s, 3H), 1.65 (s, 4H), 1.25 (s, 12H). ¹³C-NMR (75 MHz, CDCl₃) δ: 144.60, 144.06, 134.57, 130.14, 128.89, 122.12, 34.91, 34.87, 34.00, 33.91, 31.76, 31.72, 22.53.

(3,5,5,8,8-Pentamethyl-5,6,7,8-tetrahydronaphthalen-2-yl)boronic acid (15). This compound was prepared according to reference 39. A solution of 1.6 M *n*-BuLi in *n*-hexane (1.5 mL, 2.4 mmol) was

slowly added to a solution of **14** (560 mg, 2 mmol) in THF (6 mL) at -78 °C under an Ar atmosphere. The reaction mixture was stirred at -78 °C for 20 min and then a solution of triisopropyl borate (1.4 mL, 6 mmol) in THF (0.5 mL) was added to it. Stirring was continued at -78 °C for 2 h. The reaction mixture was poured into 2 M HCl aq (10 mL) and the mixture was stirred at room temperature for 1 h and diluted with EtOAc (150 mL). The organic layer was collected, washed with water (2 × 50 mL) and finally with brine (50 mL). The resulting solution was dried over MgSO₄, filtered and evaporated using a rotary evaporator. The residue was chromatographed using (SiO₂, EtOAc/n-hexane = 1/5, v/v) to yield 360 mg of **15** as a yellow oil (73%). ¹H-NMR (300 MHz, CDCl₃) δ: 8.28 (s, 1H), 7.21 (s, 1H), 2.81 (s, 3H), 1.72 (s, 4H), 1.34 (s, 6H), 1.32 (s, 6H). ¹³C-NMR (75 MHz, CDCl₃) δ: 149.42, 142.89, 141.49, 136.34, 128.59, 35.06, 35.03, 34.37, 33.82, 31.87, 31.56, 22.70.

5-Bromo-2,4-dihydroxybenzaldehyde (17). This compound was prepared according to reference 40. To a solution of 2,4-dihydroxybenzaldehyde (**16**, 3.3 g, 24 mmol) in acetic acid (24 mL) was slowly added bromine (1.24 mL, 24 mmol). The reaction mixture was stirred at room temperature for 15 h, then poured into water (35 mL), and the whole was filtered. The crude product was chromatographed (SiO₂, EtOAc/n-hexane = 1/4, v/v) and recrystallized from EtOAc/n-hexane to yield 1.46 g of **17** as pale brown needles (28%). ¹H NMR (300 MHz, CDCl₃) δ: 11.25 (s, 1H), 9.70 (d, 1H, *J* = 1 Hz), 7.66 (s, 1H), 6.63 (s, 1H), 6.11 (s, 1H).

5-Bromo-2,4-bis(methoxymethoxy)benzaldehyde (18). DIPEA (520 μL, 3 mmol) and chloromethyl methyl ether (324 μL, 4.3 mmol) were added to a solution of **17** (220 mg, 1 mmol) in DMF (3 mL) at 0 °C under an Ar atmosphere. The reaction mixture was stirred at room temperature for 27 h, then poured into sat. NH₄Cl aq (60 mL) and extracted with EtOAc (3 × 40 mL). The organic layer was collected, washed with water (2 × 60 mL) and brine (60 mL), dried over MgSO₄, and filtered. The filtrate was evaporated in a rotary evaporator. The residue was chromatographed (SiO₂, EtOAc/n-hexane = 1/5, v/v) to yield 280 mg of **18** as a white solid (92%). ¹H-NMR (300 MHz, CDCl₃) δ: 10.29 (s, 1H), 8.03 (s, 1H),

7.01 (s, 1H), 5.32 (s, 2H), 5.29 (s, 2H), 3.53 (s, 6H). ¹³C-NMR (75 MHz, CDCl₃) δ: 187.01, 160.24, 159.10, 132.36, 120.61, 105.39, 101.92, 94.75, 56.59, 56.52.

2,4-Bis(methoxymethoxy)-5-(3,5,5,8,8-pentamethyl-5,6,7,8-tetrahydronaphthalen-2-

yl)benzaldehyde (19). To a solution of **15** (200 mg, 0.8 mmol) and **18** (150 mg, 0.49 mmol) in toluene (2 mL) and ethanol (1 mL) were added tetrakis(triphenylphosphine)palladium (30 mg, 0.026 mmol) and 2 M Na₂CO₃ aq (0.5 mL). The reaction mixture was stirred at 100 °C for 24 h, then diluted with EtOAc (150 mL). The organic layer was collected, washed with sat. NH₄Cl aq (100 mL), water (100 mL) and brine (100 mL), dried over MgSO₄, and filtered. The filtrate was evaporated in a rotary evaporator. The residue was chromatographed (SiO₂, EtOAc/*n*-hexane = 1/6, v/v) to yield 180 mg of **19** as a colorless oil (86%). ¹H-NMR (300 MHz, CDCl₃) δ: 10.39 (s, 1H), 7.69 (s, 1H), 7.13 (s, 1H), 7.04 (s, 2H), 5.34 (s, 2H), 5.16 (s, 2H), 3.57 (s, 3H), 3.39 (s, 3H), 2.10 (s, 3H), 1.69 (s, 4H), 1.31 (s, 6H), 1.25 (s, 6H). ¹³C-NMR (75 MHz, CDCl₃) δ: 188.31, 160.69, 160.47, 143.81, 141.76, 134.10, 133.38, 131.20, 128.19, 127.41, 126.24, 119.63, 101.02, 94.80, 94.52, 56.55, 56.36, 35.09, 33.87, 33.79, 31.84, 31.81, 31.49, 22.56, 19.66, 14.10.

2,4-Dihydroxy-5-(3,5,5,8,8-pentamethyl-5,6,7,8-tetrahydronaphthalen-2-yl)benzaldehyde (20). To a solution of **19** (171 mg, 0.4 mmol) in EtOAc (2 mL) was added 4 M HCl/EtOAc (2 mL). The reaction mixture was stirred at room temperature for 4 h and evaporated in a rotary evaporator. The residue was chromatographed (SiO₂, EtOAc/*n*-hexane = 1/5, v/v) to yield 117 mg of **20** as a yellow solid (88%). ¹H-NMR (300 MHz, CDCl₃) δ: 11.37 (1H, s), 9.72 (1H, s), 7.32 (1H, s), 7.25 (1H, s), 7.12 (1H, s), 6.56 (1H, s), 5.52 (1H, s), 2.11 (4H, s), 1.71 (4H, s), 1.32 (6H, s), 1.27 (6H, s). ¹³C-NMR (75 MHz, CDCl₃) δ: 194.45, 163.51, 160.93, 145.77, 143.47, 135.99, 134.27, 130.69, 128.80, 128.77, 121.74, 115.19, 102.82, 60.53, 34.91, 34.05, 33.94, 31.84, 31.72, 21.02, 19.38, 14.10.

1,3-Bis(methoxymethoxy)benzene (22). This compound was prepared according to reference 41. To a suspension of 60% NaH (920 mg, 23 mmol) in DMF (10 mL) was added a solution of resorcinol (**21**, 1.1 g, 10 mmol) in DMF (10 mL). The mixture was stirred at 0 °C under an Ar atmosphere for 15 min,

then chloromethyl methyl ether (1.67 mL, 22 mmol) was added, and stirring was continued at room temperature for 27 h. The reaction mixture was poured into ice-cold water (50 mL) and extracted with EtOAc (2 × 100 mL). The organic layer was collected, washed with water (2 × 50 mL) and brine (50 mL), dried over MgSO₄, and filtered. The filtrate was evaporated in a rotary evaporator to yield 1.98 g of **22** as a clear oil (q.y.). ¹H-NMR (400 MHz, CDCl₃) δ: 7.19 (t, 1H, *J* = 8.2 Hz), 6.74 (d, 1H, *J* = 2.2 Hz), 6.70 (dd, 2H, *J* = 8.2, 2.2 Hz), 5.16 (s, 4H), 3.48 (s, 6H). ¹³C-NMR (75MHz, CDCl₃) δ: 158.17, 129.70, 109.31, 104.67, 94.12, 55.66.

(2,6-Bis(methoxymethoxy)phenyl)boronic acid (23). This compound was prepared according to reference 41. To a solution of **22** (297 mg, 1.5 mmol) in Et₂O (6 mL) was slowly added 1.6 M *n*-BuLi in *n*-hexane solution (1.13 mL, 1.8 mmol) at 0 °C under an Ar atmosphere. The reaction mixture was stirred at room temperature for 3 h, then trimethyl borate (250 μL, 2.25 mmol) was added, and stirring was continued at room temperature for 1 h. The reaction mixture was poured into 2 M HCl aq (10 mL). The whole was stirred at room temperature for 1 h. The mixture was filtered, washed with water, and dried under reduced pressure to yield 177 mg of **23** as a pale-yellow solid (49%). ¹H-NMR (300 MHz, CDCl₃) δ: 7.36 (t, 1H, *J* = 8.3 Hz), 7.23 (s, 2H), 6.88 (d, 2H, *J* = 8.3 Hz), 5.30 (s, 4H), 3.51 (s, 6H). ¹³C-NMR (75 MHz, CDCl₃) δ: 163.02, 133.00, 108.23, 94.78, 56.58.

6-(2,6-Bis(methoxymethoxy)phenyl)-1,1,4,4,7-pentamethyl-1,2,3,4-tetrahydronaphthalene (24). To a solution of **13** (113 mg, 0.4 mmol) and **23** (145 mg, 0.6 mmol) in DME (4 mL) were added tetrakis(triphenylphosphine)palladium (69 mg, 0.06 mmol), K₃PO₄ (255 mg, 1.2 mmol) and H₂O (1.3 mL). The reaction mixture was refluxed for 30 min, then poured into water (30 mL) and extracted with EtOAc (3 × 30 mL). The organic layer was collected, washed with water (2 × 50 mL) and brine (50 mL), dried over MgSO₄, and filtered. The filtrate was evaporated in a rotary evaporator. The residue was chromatographed (SiO₂, EtOAc/*n*-hexane = 1/30, v/v) to yield 124 mg of **24** as a white solid (78%). ¹H-NMR (400 MHz, CDCl₃) δ: 7.24 (t, 1H, *J* = 8.4 Hz), 7.13 (s, 1H), 7.05 (s, 1H), 6.89 (d, 2H, *J* = 8.4 Hz), 5.04 (d, 2H, *J* = 6.6 Hz), 4.96 (d, 2H, *J* = 6.6 Hz), 3.27 (s, 6H), 2.07 (s, 3H), 1.68 (s, 4H), 1.55 (s, 3H),

1.30 (s, 6H), 1.23 (s, 6H). ¹³C-NMR (75 MHz, CDCl₃) δ: 155.50, 143.21, 141.10, 133.93, 131.01, 129.93, 128.86, 128.34, 127.09, 122.91, 109.69, 109.59, 94.93, 94.43, 55.88, 35.33, 35.26, 34.92, 34.89, 33.93, 33.82, 31.93, 31.90, 31.76, 19.55.

2-(3,5,5,8,8-Pentamethyl-5,6,7,8-tetrahydronaphthalen-2-yl)benzene-1,3-diol (25). To a solution of **24** (108 mg, 0.27 mmol) was added 4 M HCl/EtOAc (2 mL). The reaction mixture was stirred at room temperature for 3 h, then poured into water (30 mL) and extracted with EtOAc (30 mL). The organic layer was collected, washed with water (30 mL) and brine (30 mL), dried over MgSO₄, and filtered. The filtrate was evaporated in a rotary evaporator. The residue was chromatographed using (SiO₂, EtOAc/*n*-hexane = 1/8, v/v) to yield 45 mg of **25** as a pale-yellow solid (54%). ¹H-NMR (300 MHz, CDCl₃) δ: 7.31 (s, 1H), 7.18 (s, 1H), 7.15 (d, 1H, *J* = 8.0 Hz), 6.59 (d, 2H, *J* = 8.0 Hz), 4.72 (s, 2H), 2.10 (s, 3H), 1.71 (s, 4H), 1.33 (s, 6H), 1.25 (s, 6H). ¹³C-NMR (75 MHz, CDCl₃) δ: 153.48, 146.69, 144.66, 144.42, 135.90, 130.16, 129.63, 129.53, 129.35, 128.91, 125.92, 114.76, 107.13, 34.95, 34.89, 34.19, 34.07, 31.88, 31.75, 31.70, 19.05.

2,4-Dihydroxy-3-(3,5,5,8,8-pentamethyl-5,6,7,8-tetrahydronaphthalen-2-yl)benzaldehyde (26). POCl₃ (100 μL) was added to DMF (350 μL) at 0 °C. The reaction mixture was stirred for 1.5 h, and then a solution of **25** (40 mg, 0.128 mmol) in DMF (1.5 mL) was added to it, and stirring was continued at room temperature for 48 h. The reaction mixture was poured into ice-cold water (30 mL), adjusted to pH 3 with sat. NaHCO₃ aq., and extracted with EtOAc (2 × 50 mL). The organic layer was washed with water (2 × 50 mL) and brine (50 mL), dried over MgSO₄, and filtered. The filtrate was evaporated in a rotary evaporator. The residue was chromatographed (SiO₂, EtOAc/*n*-hexane = 1/8, v/v) to yield 17 mg of **26** as a pale-yellow solid (39%). ¹H-NMR (300 MHz, CDCl₃) δ: 11.71 (s, 1H), 9.76 (s, 1H), 7.48 (d, 1H, *J* = 8.4 Hz), 7.28 (s, 1H), 7.11 (1H, s), 6.69 (1H, d, *J* = 8.4 Hz), 5.69 (s, 1H), 2.10 (s, 3H), 1.70 (s, 4H), 1.33 (s, 3H), 1.31 (s, 3H), 1.26 (s, 6H). ¹³C-NMR (75 MHz, CDCl₃) δ: 194.69, 161.13, 160.63, 146.03, 143.59, 135.27, 134.89, 129.18, 128.68, 125.87, 115.72, 115.10, 108.20, 35.01, 34.95, 34.14, 32.07, 31.85, 31.73, 31.69, 19.20, 14.18.

In vitro assays

Reporter gene assay. Luciferase reporter gene assays using COS-1 cells were performed according to reference 42. Briefly, COS-1 cells were transfected with three kinds of vectors consisting of human RXR receptor alpha, a luciferase reporter gene under the control of the appropriate RXR response element (CRBP_{II}-tk-Luc), and secreted alkaline phosphatase (SEAP) gene as a background. Test compound solutions (DMSO concentration: 1%) were added to a suspension of transfected cells seeded at about 2.0×10^4 cells/well in 96-well white plates. After incubation in a humidified atmosphere of 5% CO₂ at 37°C for 24 h, 25 µL of the medium was used for analysis of SEAP activity, and the remaining cells were used for luciferase reporter gene assays with a Steady-Glo Luciferase Assay system (Promega) according to the supplier's protocol. The luciferase activities were normalized using the SEAP activities. The assays were carried out three times in triplicate.

Ligand binding assay using radioligand. Competitive binding assay using 9-*cis*-[11,12-³H]-retinoic acid ([³H]**1**) was performed as described in references 43 and 44 with some modifications. [³H]**1**, NET1151, 1.11–2.22 TBq/mmol (30–60 Ci/mmol) 7.4 MBq/mL (0.2 mCi/mL)) was purchased from PerkinElmer (USA). hRXR α -LBD (NR2B1, Catalog No: 31135) was purchased from Active Motif, Inc (USA). Dextran-coated charcoal (DCC) was purchased from Sigma-Aldrich. Assay buffer contained 20 mM Tris-HCl (pH 7.5), 150 mM NaCl, 1 mM EDTA, 5 mM dithiothreitol (DTT), 10% glycerol. hRXR α -LBD, **3**, and [³H]**1** were diluted as required with the assay buffer described above.

K_d determination of [³H]1**.** To a 1.5 mL Eppendorf tube were added 30 µL of serial dilutions of hRXR α -LBD (3,000 nM to 3 nM, common ratio 3, 12 final concentration levels), 15 µL of 2% DMSO assay buffer or 40 µM bexarotene (final concentration 10 µM), and 15 µL of 40 nM [³H]**1** (final concentration was 10 nM). Three samples per test condition were used. The mixture was incubated at 4°C overnight. [³H]**1** bound to hRXR α -LBD was separated from free [³H]**1** by adding 20 µL of ice-cold 0.4% DCC suspension to each sample. The samples were placed on ice for 1 min and the reaction mixture was centrifuged at 12,000 rpm (8,000×g) at 4°C for 5 min. Fifty microliters of each supernatant

was poured into a scintillation vial containing 3 mL scintillation cocktail and bound radioactivity was determined by liquid scintillation counting of the solution. The specific equilibrium binding constant (K_d) was derived from the specific binding curve by fitting the data into a sigmoid equation using Excel software. The K_d value of [^3H]**1** was obtained as 37 nM. The concentration of hRXR α -LBD was 50 nM.

IC₅₀ determination of test compounds using [^3H]**1**. To a 1.5 mL Eppendorf tube were added 30 μL of 100 nM hRXR α -LBD, 15 μL of serial dilutions of test compounds (10,000 nM to 1 nM, common ratio 3, 9 final concentration levels) in assay buffer containing 8% DMSO, and 15 μL of 40 nM [^3H]**1** (final concentration 10 nM). Three samples per test condition were used. The mixture was incubated at 4°C overnight, and bound radioligand was separated from free as described above. IC_{50} was derived from the binding curve by fitting the data to a sigmoid equation using Excel software. The inhibition constant (K_i) value was calculated as described below.

K_i calculation from IC₅₀. The inhibition constant (K_i) value of each test compound was calculated by using equation 1.³¹

$$K_i = \text{IC}_{50} / (1 + [\text{L}] / K_d) \text{ ----- (1)}$$

where IC_{50} is the concentration of test compound that inhibits 50% of binding, $[\text{L}]$ is the concentration of [^3H]**1** or **10** used, and K_d is the K_d value of [^3H]**1** or **10**.

ASSOCIATED CONTENT

Supporting Information

The Supporting Information is available free of charge on the ACS Publications website at DOI:

Crystallization and X-ray data collection of hRXR α -LBD/**10**, UV-vis and fluorescence spectra measurements, fluorescence quantum yield determination, K_d determination of CU-6PMN (**10**), transformation of measured fluorescence intensity into bound receptor concentration, binding affinity

assay of a panel of RXR ligands with hRXR α -LBD using CU-6PMN (**10**), Z'-factor, statistical analysis, chemical structures of the compounds used, absorbance and fluorescent spectra, binding assay protocol, NMR spectra, HPLC charts (PDF).

Molecular formula strings and some data (CSV).

Atomic coordinates of hRXR α -LBD/**10** (PDB ID: 6JNO) by binding mode analysis (PDB). The atomic coordinates will be released when the article is published.

AUTHOR INFORMATION

Corresponding Author

* Hiroki Kakuta (kakuta-h@okayama-u.ac.jp; phone: +81-(0)86-251-7963)

* Shogo Nakano (snakano@u-shizuoka-ken.ac.jp; phone: +81-(0)54-264-5576)

ORCID

Makoto Makishima: 0000-0002-4630-905X

Sohei Ito: 0000-0002-9937-3100

Hiroaki Tokiwa: 0000-0002-3790-1799

Shogo Nakano: 0000-0002-6614-7158

Hiroki Kakuta: 0000-0002-3633-8121

Author Contributions

S.Y., M.W. and H.K. conceived and designed the project. S.Y., M.W., and Y.T. synthesized compounds. M.K., S.N., and T.M. produced hRXR α -LBD. S.Y. and M.F. performed reporter gene assays. S.Y., M.W., Y.T., and H.K. performed RI binding assay. M.K., S.N., T.M., and S.I. performed X-ray structure analysis. S.Y., M.T. and M.F. analyzed UV and fluorescence spectra. S.Y. and M.F. performed fluorescence-based binding assay. All authors analyzed and discussed the data. The manuscript was written by S.Y., M.W., M.K., Y.T., S.N., and H.K.

Funding Sources

This work was partially supported by Grant-in-Aid from the Japan Society for the Promotion of Science (JSPS) (to S.Y.), JSPS KAKENHI Grant Numbers 16K18688, 18K14391 (to S.N.) and 17K06931(to S.I.), Okayama Foundation for Science and Technology (to H.K.), and The Tokyo Biochemical Research Foundation (TBRF) (to H.K.).

Notes

The authors declare the following competing financial interest: The patent applications PCT/JP2016/085729 and WO2017094838A1 included results from this article. This research was partially performed in collaboration with AIBIOS Co., Ltd.. Michiko Fujihara was an employee of AIBOS. No other author reports any potential conflict of interest relevant to this article.

ACKNOWLEDGMENT

The authors are grateful to the Division of Instrumental Analysis, Okayama University for the NMR and MS measurements. We would like to thank Dr. Tomoya Hirano (Osaka University of Pharmaceutical Sciences, Takatsuki, Osaka, Japan) for his helpful advice on quantum yield measurement. The authors thank Dr. Hiroyuki Kagechika (Tokyo Medical and Dental University, Tokyo, Japan), for providing PA452 and HX531.

ABBREVIATIONS

Abs, absorption; ACN, acetonitrile; DHA, docosahexaenoic acid; DTT, dithiothreitol; EPA, eicosapentaenoic acid; Em, emission; Ex, excitation; Fl, fluorescence; HPLC, high performance liquid chromatography; hRXR, human RXR; LBD, ligand-binding domain; LBP, ligand-binding pocket; LXR, liver X receptor; MS, mass spectrometry; Nurr1, nuclear receptor related 1 protein; PPAR, peroxisome proliferator activated receptor; RAR, retinoic acid receptor; RI, radioisotope; RXR, retinoid X receptor; SD, standard deviation; TR-FRET, time-resolved fluorescence resonance energy transfer.

REFERENCES

- (1) Evans, R.M.; Mangelsdorf, D.J. Nuclear receptors, RXR, and the big bang. *Cell* **2014**, *157*, 255–266.
- (2) Huang, P.; Chandra, V.; Rastinejad, F. Structural overview of the nuclear receptor superfamily: insights into physiology and therapeutics. *Annu. Rev. Physiol.*, **2010**; *72*, 247–272.
- (3) Mukherjee, R.; Davies, P.J.; Crombie, D.L.; Bischoff, E.D.; Cesario, R.M.; Jow, L.; Hamann, L.G.; Boehm, M.F.; Mondon, C.E.; Nadzan, A.M.; Paterniti, J.R.Jr; Heyman, R.A. Sensitization of diabetic and obese mice to insulin by retinoid X receptor agonists. *Nature* **1997**, *386*, 407–410.
- (4) Heyman R.A.; Mangelsdorf, D.J.; Dyck, J.A.; Stein, R.B.; Eichele, G.; Evans, R.M.; Thaller, C. 9-*cis* retinoic acid is a high affinity ligand for the retinoid X receptor. *Cell* **1992**, *68*, 397–406.
- (5) Arnold, S.L.; Amory, J.K.; Walsh, T.J.; Isoherranen, N. A sensitive and specific method for measurement of multiple retinoids in human serum with UHPLC-MS/MS. *J. Lipid Res.* **2012**, *53*, 587–598.
- (6) Rühl, R.; Krzyżosiak, A.; Niewiadomska-Cimicka, A.; Rochel, N.; Szeles, L.; Vaz, B.; Wietrzych-Schindler, M.; Álvarez, S.; Szklenar, M.; Nagy, L.; de Lera, A.R.; Krężel, W.; 9-*cis*-13,14-Dihydroretinoic acid is an endogenous retinoid acting as RXR ligand in mice. *PLoS Genet.*, **2015**, *11*, e1005213.
- (7) Shen, D.; Yu, X.; Wu, Y.; Chen, Y.; Li, G.; Cheng, F.; Xia, L. Emerging roles of bexarotene in the prevention, treatment and anti-drug resistance of cancers. *Expert Rev. Anticancer. Ther.*, **2018** *18*, 487–499.
- (8) Cramer, P.E.; Cirrito, J.R.; Wesson, D.W.; Lee, C.Y.; Karlo, J.C.; Zinn, A.E.; Casali, B.T.; Restivo, J.L.; Goebel, W.D.; James, M.J.; Brunden, K.R.; Wilson, D.A.; Landreth, G.E. ApoE-directed therapeutics rapidly clear β -amyloid and reverse deficits in AD mouse models. *Science* **2012**, *335*, 1503–1506.

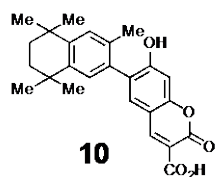
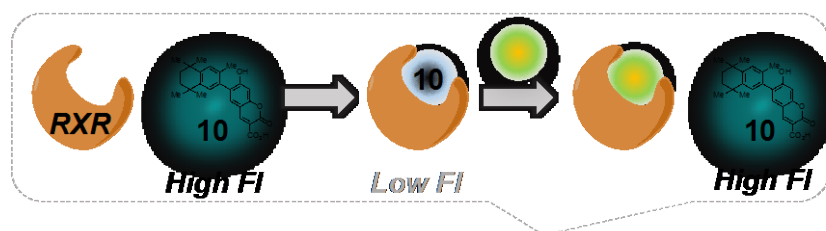
- (9) Dheer, Y.; Chitranshi, N.; Gupta, V.; Abbasi, M.; Mirzaei, M.; You, Y.; Chung, R.; Graham, S.L.; Gupta, V. Bexarotene modulates retinoid-X-receptor expression and is protective against neurotoxic endoplasmic reticulum stress response and apoptotic pathway activation. *Mol. Neurobiol.*, **2018**, *55*, 9043–9056.
- (10) McFarland, K.; Spalding, T.A.; Hubbard, D.; Ma, J.N.; Olsson, R.; Burstein, E.S. Low dose bexarotene treatment rescues dopamine neurons and restores behavioral function in models of Parkinson's disease. *ACS Chem. Neurosci.*, **2013**, *4*, 1430–1438.
- (11) Friling, S.; Bergsland, M.; Kjellander, S. Activation of retinoid X receptor increases dopamine cell survival in models for Parkinson's disease. *BMC Neurosci.*, **2009**, *10*, 146.
- (12) Pérez, E.; Bourguet, W.; Gronemeyer, H.; de Lera, A.R. Modulation of RXR function through ligand design. *Biochim. Biophys. Acta.*, **2012**, *821*, 57–69.
- (13) de Urquiza, A.M.; Liu, S.; Sjöberg, M.; Zetterström, R.H.; Griffiths, W.; Sjövall, J.; Perlmann, T. Docosahexaenoic acid, a ligand for the retinoid X receptor in mouse brain. *Science* **2000**, *290*, 2140–2144.
- (14) Lengqvist, J.; Mata De Urquiza, A.; Bergman, A.C.; Willson, T.M.; Sjövall, J.; Perlmann, T.; Griffiths, W.J. Polyunsaturated fatty acids including docosahexaenoic and arachidonic acid bind to the retinoid X receptor alpha ligand-binding domain. *Mol. Cell Proteomics.*, **2004**, *3*, 692–703.
- (15) Zehr, K.R.; Walker, M.K.; Omega-3 polyunsaturated fatty acids improve endothelial function in humans at risk for atherosclerosis: A review. *Prostaglandins Other. Lipid Mediat.*, **2018** *134*, 131–140.
- (16) Balaguer, P.; Delfosse, V.; Grimaldi, M.; Bourguet, W. Structural and functional evidences for the interactions between nuclear hormone receptors and endocrine disruptors at low doses. *C. R. Biol.* **2017**, *340*, 414–420.

- (17) Stafslie, D.K.; Vedvik, K.L.; De Rosier, T.; Ozers, M.S. Analysis of ligand-dependent *recruitment* of coactivator peptides to RXRbeta in a time-resolved fluorescence resonance energy transfer assay. *Mol Cell Endocrinol.* **2007**, *264*, 82–89.
- (18) Allenby, G.; Bocquel, M.T.; Saunders, M.; Kazmer, S.; Speck, J.; Rosenberger, M.; Lovey, A.; Kastner, P.; Grippo, J.F.; Chambon, P.; Levin, A.A. Retinoic acid receptors and retinoid X receptors: interactions with endogenous retinoic acids. *Proc. Natl. Acad. Sci. U S A.* **1993**, *90*, 30–34.
- (19) Cheng, L.; Norris, A.W.; Tate, B.F.; Rosenberger, M.; Grippo, J.F.; Li, E. Characterization of the ligand binding domain of human retinoid X receptor alpha expressed in *Escherichia coli*. *J. Biol. Chem.*, **1994**, *269*, 18662–18667.
- (20) van de Weert, M. Fluorescence quenching to study protein-ligand binding: common errors. *J. Fluoresc.*, **2010**, *20*, 625–629.
- (21) Shiizaki, K.; Yoshikawa, T.; Takada, E.; Hirose, S.; Ito-Harashima, S.; Kawanishi, M.; Yagi, T. Development of yeast reporter assay for screening specific ligands of retinoic acid and retinoid X receptor subtypes. *J. Pharmacol. Toxicol. Methods.* **2014**, *69*, 245–252.
- (22) Liu, D.; Guo, J.; Luo, Y.; Broderick, D.J.; Schimerlik, M.I.; Pezzuto, J.M.; van Breemen, R.B. Screening for ligands of human retinoid X receptor-alpha using ultrafiltration mass spectrometry. *Anal. Chem.* **2007**, *79*, 9398–9402.
- (23) Rush, M.D.; Walker, E.M.; Prehna, G.; Burton, T.; van Breemen, R.B. Development of a magnetic microbead affinity selection screen (MagMASS) using mass spectrometry for ligands to the retinoid X receptor- α . *J. Am. Soc. Mass Spectrom.* **2017**, *28*, 479–485.
- (24) Xu, D.; Cai, L.; Guo, S.; Xie, L.; Yin, M.; Chen, Z.; Zhou, H.; Su, Y.; Zeng, Z.; Zhang, X. Virtual screening and experimental validation identify novel modulators of nuclear receptor RXR α from Drugbank database. *Bioorg. Med. Chem. Lett.* **2017**, *27*, 1055–1061.

- (25) Yamada, S.; Ohsawa, F.; Fujii, S.; Shinozaki, R.; Makishima, M.; Naitou, H.; Enomoto, S.; Tai, A.; Kakuta, H. Fluorescent retinoid X receptor ligands for fluorescence polarization assay. *Bioorg. Med. Chem. Lett.* **2010**, *20*, 5143–5146.
- (26) Tomlinson, C.W.E.; Chisholm, D.R.; Valentine, R.; Whiting, A.; Pohl, E. Novel fluorescence competition assay for retinoic acid binding proteins. *ACS. Med. Chem. Lett.* **2018**, *9*, 1297–1300.
- (27) Chisholm, D.R.; Tomlinson, C.W.E.; Zhou, G.L.; Holden, C.; Affleck, V.; Lamb, R.; Newling, K.; Ashton, P.; Valentine, R.; Redfern, C.; Erostyák, J.; Makkai, G.; Ambler, C.A.; Whiting, A.; Pohl, E. Fluorescent retinoic acid analogues as probes for biochemical and intracellular characterization of retinoid signaling pathways. *ACS Chem. Biol.* **2019**, *14*, 369–377.
- (28) Aaron, J.J.; Buna, M.; Parkanyi, C.; Antonious, M.S.; Tine, A.; Cisse, L. Quantitative treatment of the effect of solvent on the electronic absorption and fluorescence spectra of substituted coumarins: Evaluation of the first excited singlet-state dipole moments. *J. Fluoresc.* **1995**, *5*, 337–347.
- (29) Sherman, W.R.; Robins, E. Fluorescence of substituted 7-hydroxycoumarins. *Anal. Chem.* **1968**, *40*, 803–805.
- (30) Nahoum, V.; Pérez, E.; Germain, P.; Rodríguez-Barrios, F.; Manzo, F.; Kammerer, S.; Lemaire, G.; Hirsch, O.; Royer, C.A.; Gronemeyer, H.; de Lera, A.R.; Bourguet, W. Modulators of the structural dynamics of the retinoid X receptor to reveal receptor function. *Proc. Natl. Acad. Sci. U S A.* **2007**, *104*, 17323–17328.
- (31) Cheng, Y.; Prusoff, W.H. Relationship between the inhibition constant (K_i) and the concentration of inhibitor which causes 50 per cent inhibition (I_{50}) of an enzymatic reaction. *Biochem. Pharmacol.*, **1973**, *22*, 3099–3108.

- (32) Xia, G.; Boerma, L.J.; Cox, B.D.; Qiu, C.; Kang, S.; Smith, C.D.; Renfrow, M.B.; Muccio, D.D. Structure, energetics, and dynamics of binding coactivator peptide to the human retinoid X receptor α ligand binding domain complex with 9-*cis*-retinoic acid. *Biochemistry* **2011**, *50*, 93–105.
- (33) Zhang, H.; Chen, L.; Chen, J.; Jiang, H.; Shen, X. Structural basis for retinoic X receptor repression on the tetramer. *J. Biol. Chem.* **2011**, *286*, 24593–24598.
- (34) Chen, L.; Aleshin, A.E.; Alitongbieke, G.; Zhou, Y.; Zhang, X.; Ye, X.; Hu, M.; Ren, G.; Chen, Z.; Ma, Y.; Zhang, D.; Liu, S.; Gao, W.; Cai, L.; Wu, L.; Zeng, Z.; Jiang, F.; Liu, J.; Zhou, H.; Cadwell, G.; Liddington, R.C.; Su, Y.; Zhang, X.K. Modulation of nongenomic activation of PI3K signalling by tetramerization of *N*-terminally-cleaved RXR α . *Nat. Commun.* **2017**, 16066.
- (35) Chen, L.; Wang, Z.G.; Aleshin, A.E.; Chen, F.; Chen, J.; Jiang, F.; Alitongbieke, G.; Zeng, Z.; Ma, Y.; Huang, M.; Zhou, H.; Cadwell, G.; Zheng, J.F.; Huang, P.Q.; Liddington, R.C.; Zhang, X.K.; Su, Y. Sulindac-derived RXR α modulators inhibit cancer cell growth by binding to a novel site. *Chem. Biol.* **2014**, *21*, 596–607.
- (36) Ohno, K.; Fukushima, T.; Santa, T.; Waizumi, N.; Tokuyama, H.; Maeda, M.; Imai, K. Estrogen receptor binding assay method for endocrine disruptors using fluorescence polarization. *Anal. Chem.* **2002**, *74*, 4391–4396.
- (37) Goldstein, J.T.; Dobrzyn, A.; Clagett-Dame, M.; Pike, J.W.; DeLuca, H.F. Isolation and characterization of unsaturated fatty acids as natural ligands for the retinoid-X receptor. *Arch. Biochem. Biophys.* **2003**, *420*, 185–193.
- (38) Zou, Y.; Qin, L.; Ren, X.; Lu, Y.; Li, Y.; Zhou, J.S. Selective arylation and vinylation at the α position of vinylarenes. *Chem. Eur. J.*, **2013**, *19*, 3504–3511.
- (39) Jurutka, P.W.; Kaneko, I.; Yang, J.; Bhogal, J.S.; Swierski, J.C.; Tabacaru, C.R.; Montano, L.A.; Huynh, C.C.; Jama, R.A.; Mahelona, R.D.; Sarnowski, J.T.; Marcus, L.M.; Quezada, A.; Lemming, B.; Tedesco, M.A.; Fischer, A.J.; Mohamed, S.A.; Ziller, J.W.; Ma, N.; Gray, G.M.; van der Vaart,

- A.; Marshall, P.A.; Wagner, C.E. Modeling, synthesis, and biological evaluation of potential retinoid X receptor (RXR) selective agonists: novel analogues of 4-[1-(3,5,5,8,8-pentamethyl-5,6,7,8-tetrahydro-2-naphthyl)ethynyl]benzoic acid (bexarotene) and (E)-3-(3-(1,2,3,4-tetrahydro-1,1,4,4,6-pentamethylnaphthalen-7-yl)-4-hydroxyphenyl)acrylic acid (CD3254). *J. Med. Chem.*, **2013**, *56*, 8432–8454.
- (40) Liu, Z.; Lee, W.; Kim, S.N.; Yoon, G.; Cheon, S.H. Design, synthesis, and evaluation of bromo-retrochalcone derivatives as protein tyrosine phosphatase 1B inhibitors. *Bioorg. Med. Chem. Lett.*, **2011**, *21*, 3755–3758.
- (41) Mori, K.; Ichikawa, Y.; Kobayashi, M.; Shibata, Y.; Yamanaka, M.; Akiyama, T. Enantioselective synthesis of multisubstituted biaryl skeleton by chiral phosphoric acid catalyzed desymmetrization/kinetic resolution sequence. *J. Am. Chem. Soc.* **2013**, *135*, 3964–3970.
- (42) Kakuta, H.; Yakushiji, N.; Shinozaki, R.; Ohsawa, F.; Yamada, S.; Ohta, Y.; Kawata, K.; Nakayama, M.; Hagaya, M.; Fujiwara, C.; Makishima, M.; Uno, S.; Tai, A.; Maehara, A.; Nakayama, M.; Oohashi, T.; Yasui, H.; Yoshikawa, Y. RXR partial agonist CBt-PMN exerts therapeutic effects on type 2 diabetes without the side effects of RXR full agonists. *ACS Med. Chem. Lett.* **2012**, *3*, 427–432.
- (43) Allenby, G.; Bocquel, M.T.; Saunders, M.; Kazmer, S.; Speck, J.; Rosenberger, M.; Lovey, A.; Kastner, P.; Grippo, J.F.; Chambon, P. Retinoic acid receptors and retinoid X receptors: interactions with endogenous retinoic acids. *Proc. Natl. Acad. Sci. U S A.* **1993**, *90*, 30–34.
- (44) A. A. Levin, L. J. Sturzenbecker, S. Kazmer, T. Bosakowski, C. Huselton, G. Allenby, J. Speck, C. Kratzeisen, M. Rosenberger, A. Lovey, J. F. Grippo, 9-Cis retinoic acid stereoisomer binds and activates the nuclear receptor RXR α . *Nature* **1992**, *355*, 359–361.



Binding assay for RXR ligands

- General fluorescent plate reader (Ex 360/Em 465)
 - Within 3 hours (including sample preparation)
 - No Bound/Free separation
-